Amperometric measurements of catecholamine release from single vesicles in MN9D cells

Yan Dong[*,†], **Michael L. Heien**[*], **Marc M. Maxson**[‡], and **Andrew G. Ewing**[*,§,¶]

[*] *Department of Chemistry, The Pennsylvania State University, University Park, Pennsylvania, USA*

[†] *Department of Neurosurgery, Changzheng Hospital, Second Military Medical University, Shanghai, China*

[‡] *Huck Institutes of the Life Sciences, The Pennsylvania State University, University Park, Pennsylvania, USA*

[§] *Department of Neural and Behavioral Sciences, The Pennsylvania State University College of Medicine, Hershey, Pennsylvania, USA*

[¶] *Department of Chemistry, Göteborg University, Göteborg, Sweden*

Abstract

MN9D cells have been used as a successful model to investigate dopamine pharmacology and to test the specific effects of drugs for the treatment of Parkinson's disease. However, quantitative measurements of quantal release from these cells have not been carried out. In this work, we used amperometry to investigate catecholamine release from MN9D cells. Amperometric events were observed in both undifferentiated and differentiated (butyric acid-treated) cells. An increase in quantal size and half-width was observed for differentiated cells versus undifferentiated cells; however, the number of events per cell and the amplitude remained constant. In transmission electron microscopy images, no obvious cluster of small synaptic vesicles was observed, and large dense-core vesicles were present in the cell body of undifferentiated cells; however, after differentiation, vesicles were concentrated in the cell processes. In differentiated cells, L-DOPA caused an increase in quantal size and half-width, which could be blocked by the vesicular monoamine transporter inhibitor, reserpine.

Keywords

catecholamine; dopamine; half-width; MD9D cells; Parkinson's disease; quantal size

---

The dopaminergic neurons in the substantia nigra and ventral tegmental area that give rise to the nigrostriatal and mesocorticolimbic projections play a critical role in the central regulation of motor and motivational functions (Björklund and Dunnett 2007). Mesocorticolimbic/nigrostriatal dysfunction underlies Parkinson's disease (PD), schizophrenic psychosis, tardive dyskinesia, drug dependence, and forms of dementia (Iversen and Iversen 2007). These functions are largely mediated by the release of dopamine (DA) from axon terminals in the striatum and cortex. Release of catecholamines such as DA can be studied both *in vivo* and *in vitro* with carbon-fiber microelectrodes (Westerink and Ewing 2008; Robinson *et al.* 2003). Electrochemical detection can be carried out in one of two measurement modes: fast-scan cyclic voltammetry or amperometry. The characteristic voltammograms of different

---

neurotransmitters obtained by fast-scan cyclic voltammetry provide qualitative information, while amperometry provides quantitative information with greater sensitivity.

Many different types of brain-related cells, including bovine adrenal cells, PC12 cells, invertebrate neurons, peripheral neurons, and midbrain dopaminergic neurons have been used in amperometric studies to probe the process of neurotransmission (Sombers *et al.* 2004; Colliver *et al.* 2001; Zhang *et al.* 2008; Bruns *et al.* 2000; Pothos *et al.* 1998a,b). Among these cells, PC12 cells are commonly used to study catecholamine release. However, undifferentiated PC12 cells apparently function as endocrine cells, but not as nerve cells, whereas differentiated PC12 cells show some characteristics of sympathetic neurons. To create a better model of a dopaminergic cell, a cell line (MN9D) was generated by somatic cell fusion of primary neurons from mouse embryonic Day 14 rostral mesencephalic tegmentum and the neuroblastoma cell line, N18TG2 (Choi *et al.* 1991). The resultant cells express tyrosine hydroxylase, release and transport DA, express voltage-activated sodium channels, and are sensitive to the dopaminergic cell toxin, MPP^+ (Choi *et al.* 1991; Chen *et al.* 2005). The cell line shows neuronal properties including catecholamine-specific histofluorescence, neurite formation with immunoreactivity to neurofilament proteins, and large voltage-sensitive sodium currents with the generation of action potentials (Choi *et al.* 1991). MN9D cells can release both DA and norepinephrine (NA). Previous studies have quantified NA levels in the supernatant by both HPLC and gas chromatography–mass spectroscopy and determined the NA content, which is approximately 15% of the DA levels (Choi *et al.* 1991). These cells are commonly used to test mechanisms and potential therapeutics relevant to the loss of dopaminergic neurons in PD (Lee *et al.* 2008; Cavanaugh *et al.* 2006). PD is characterized by the degeneration of dopaminergic neurons in the nigrostriatal system and the symptoms can be alleviated by DA replacement using L-DOPA. Current treatment strategies focus on replacement of lost dopaminergic neurons or increasing DA release from surviving neurons. To date, modest work has been carried out to study the release of catecholamines from single vesicles in MN9D cells.

In the present study, we adopted amperometric methods to investigate the characteristics of vesicular quantal release in MN9D dopaminergic cells. Upon differentiation with butyric acid, differentiated MN9D cells produce an increased quantal size compared with undifferentiated MN9D cells. The number of molecules released per quanta can be modulated by changes in neurotransmitter synthesis. Transmission electron microscopy data indicate that neurotransmitters are stored in large dense-core vesicles (LDCV). The data presented here demonstrate that amperometry can be used to quantify release from MN9D cells and that these cells are a useful cell model to investigate the effects and underlying mechanisms of drugs on quantal release of DA. These cells partially bridge the gap between pheochromocytoma cells and dopaminergic neurons, making them an attractive system to test experimental paradigms. Furthermore, we show that the quantal size during exocytosis increases for differentiated cells compared with undifferentiated cells in this model, which could have important implications in the interpretation of drug treatments.

Material and methods

Cell culture

MN9D cells were obtained from Dr. A. Heller (University of Chicago, Chicago, IL, USA). Cells were maintained in Dulbecco's modified Eagle's medium (D5648; Sigma, St Louis, MO, USA) supplemented with 10% (v/v) heat-inactivated fetal bovine serum (Hyclone, Logan, UT, USA), 3.7 g/L $NaHCO_3$, 50 U/mL penicillin, and 50 μg/mL streptomycin (Gibco, Rockville, MD, USA) in an incubator with an atmosphere of 7% CO_2 at 37°C. Cells were grown in poly-D-lysine flasks (BD, Franklin Lakes, NJ, USA). Differentiation of MN9D cells was performed by exposing cells to 1 mM butyric acid for at least 6 days. Media was replaced every 48 h.

Electrochemical recording

Carbon-fiber microelectrodes (5-μm diameter) were constructed as described previously (Robinson *et al.* 2003) and back-filled with 3 M KCl. Electrode tips were polished at 45° angle on a diamond dust-embedded micropipette beveling wheel (Model BV-10; Sutter Instrument, Novato, CA, USA). Cyclic voltammograms were generated for each electrode in a nitrogen-saturated 0.1 mM DA solution (in 0.1 M phosphate-buffered saline, pH 7.4), and only electrodes with stable I–E curves were used. Amperometric recordings were made as described previously (Sombers *et al.* 2004). The output was filtered at 2 kHz using a four-pole low-pass Bessel filter and digitized at 5 kHz. Data were displayed in real time and stored in the computer with no further filtering. Exocytosis was stimulated at 40-s intervals with a 5-s, 20-psi pulse (Picospritzer II; General Valve, Fairfield, NJ, USA) of physiological saline with elevated potassium (100 mM KCl). All experiments were performed at $37 \pm 1°C$. Exocytotic spikes were identified (> five times the noise), and the spike characteristics – area (pC), $t_{1/2}$ (ms), and I_{max} (pA) – were determined using a multipass algorithm described previously (Mosharov and Sulzer 2005). The 40-s interval after each stimulus was analyzed for exocytotic spikes (every event was counted). The area of each amperometric spike is directly proportional to the number of molecules detected from a single vesicle by the relationship, $Q = nNF$, where Q is the charge of each current transient, N is the number of moles, F is Faraday's constant (96 485 C/equiv), and n is the number of electrons transferred per oxidized molecules (this was assumed to be two for catecholamines). Signals were designated as spikes if their I_{max} values were five times the noise (typically 0.6 pA) of a 1-s portion of stable baseline recorded before the first stimulation. All peaks identified by the program were inspected visually, and overlapping peaks were excluded manually from the datasets.

Transmission electron microscopy

Cells seeded in poly-D-lysine culture slides (BD) were fixed with an ice-cold fixative containing 2% glutaraldehyde in 0.1 M phosphate buffer, pH 7.4 for 2 h, and then post-fixed in 1% OsO_4 for 1 h. The cells were dehydrated by serial treatment in solutions of graded ethanol and embedded in Eponite 12. The areas of interest were selected under a dissecting microscope and 80-nm-thick sections were produced in an ultramicrotome (Reichart Microscopy, Depew, NY, USA). Sections were contrast enhanced with uranyl acetate and lead citrate and examined with a JEOL JEM 1200 EXII transmission electron microscope (JEOL, Peabody, MA, USA) at 80 kV.

Quantitative analysis of vesicle structures was performed using Image J 1.37v (Wayne Rasband, NIH, Bethesda, MD, USA). Transmission electron microscopy images were imported into this software, and the limiting membrane of each vesicle as well as the perimeter of its dense core were traced. Once each object was inscribed, Image J determined its diameter (the average distance of the major and minor axis on the initial trace). Only vesicles in which a dense core could be clearly identified were measured.

Statistics

Comparison of populations used the Kolmogorov–Smirnov statistic (Mini Analysis Program by Synaptosoft, Version 6.0.3; Synaptosoft, Decatur, MA, USA), a standard non-parametric procedure used for the analysis of quantal populations detected by post-synaptic recording. The number of events and the size of dense cores and halos were tested for significant differences by using Student's *t*-test. Results were considered significant if associated *p*-values were less than 0.05. All values are reported as the mean ± SEM.

Results

Exocytosis from undifferentiated and differentiated MN9D cells

MN9D cells display many of the characteristics of dopaminergic neurons. When maintained in Dulbecco's modified Eagle's medium, they remain undifferentiated showing a non-neuronal morphology with a round cell body generally lacking any process extension (Fig. 1a). In the presence of butyric acid (more than 6 days in culture), these cells differentiate by flattening the cell body and extending processes (Fig. 1b).

To directly observe quantal release from MN9D cells, electrodes were placed on the surface of an undifferentiated MN9D cells (cultured for 5 days, Fig. 1c) or the process terminals of differentiated MN9D cells (cultured for 7–13 days, Fig. 1d). Although the differentiated cells are older, we assume differences are as a result of differentiation, but in any case the important issue is that when differentiated and undifferentiated cells are used under the conditions and ages reported, there are distinct differences in release and vesicle morphology. Fourteen percent of undifferentiated cells (30 out of 220 cells) showed amperometric events in response to high potassium stimulation. After exposure to butyric acid, 34% of differentiated cells (18 out of 53 cells) displayed amperometric events. Depolarization by high potassium generally evoked low numbers of amperometric events (2.73 ± 0.8 events for undifferentiated cells, 5.94 ± 2.76 events for differentiated cells, $p > 0.05$). Example data from the undifferentiated and differentiated MN9D cells are shown in Fig. 1e. The quantal size for the stimulus secretion events has been determined by evaluating the area under each current transient, which corresponds to the charge detected for the oxidation of the contents of a single vesicle. Quantal size in differentiated MN9D cells evoked by high K^+ was increased to $156 \pm 14\%$ of the undifferentiated MN9D cells (from $31.6 \times 10^3 \pm 2.8 \times 10^3$ to $49.3 \times 10^3 \pm 4.2 \times 10^3$ molecules). The spike amplitude was not affected by treatment with *n*-butyric acid. Quantal sizes from both undifferentiated and differentiated MN9D cells are shown in Fig. 2. Only one population of quantal size is present in both undifferentiated and differentiated MN9D cells as the normal probability plot of cube root transforms of the quantal sizes can be modelled with one line (Sulzer and Pothos 2000). Amperometric events were detected in the cell bodies of undifferentiated cells and the process terminals of differentiated cells; moreover, amperometric events were also detected in the cell bodies of differentiated cells (data are not shown), although these events were rare (observed in 3 of 87 cells).

Distribution of vesicles in undifferentiated and differentiated MN9D cells

The typical ultrastructural features of undifferentiated and differentiated MN9D cells are shown in Fig. 3. LDCVs were present in the cell body of undifferentiated MN9D cells (Fig. 3c). When MN9D cells were differentiated, LDCVs mainly accumulated in the process, existing sparsely in the cell body (Fig. 3a and b). No obvious clusters of small synaptic vesicles (SSVs) were observed in both undifferentiated and differentiated MN9D cells.

The sizes of vesicles, dense cores, and halos were measured in the cell bodies of seven undifferentiated cells and in the processes of eight differentiated cells. The sizes of vesicles in both types of cells are similar (109 ± 3 nm for undifferentiated cells; $n = 52$ vesicles, 106 ± 3 nm for differentiated cells; $n = 63$ vesicles, $p > 0.05$), while undifferentiated cells have relatively larger dense cores (83 ± 3 nm for undifferentiated cells; $n = 52$ vesicles, 70 ± 3 nm for differentiated cells; $n = 63$ vesicles, $p < 0.01$) and smaller halos compared with differentiated cells (26 ± 0.8 nm for undifferentiated cells; $n = 52$ vesicles, 36 ± 1 nm for differentiated cells; $n = 63$ vesicles, $p < 0.01$).

VMAT-mediated changes in exocytosis from differentiated MN9D cells

L-DOPA, a precursor of DA, is converted to DA by the cytosolic enzyme aromatic L-amino acid decarboxylase. A summary of amperometric events from differentiated MN9D cells with DA pharmacology is exhibited in Fig. 4. The quantal size and half-width values increased significantly for differentiated MN9D cells exposed to 100 μM L-DOPA for 90 min at 37°C. However, the change in amplitude was not significant when compared with the control group. When differentiated MN9D cells were incubated for 90 min at 37°C with 100 nM reserpine, a potent inhibitor of the vesicular monoamine transporter (VMAT), there was a significant decrease in quantal size and half-width. In contrast to the effects independently elicited by both drugs, when differentiated MN9D cells were exposed simultaneously to 100 μM L-DOPA and 100 nM reserpine for 90 min at 37°C, amperometric characteristics were not significantly different from those in the control group (Fig. 4).

Discussion

We show that differentiated MN9D cells demonstrated increased quantal size and half-width when compared with undifferentiated cells. It appears that cell differentiation alters the average amount of catecholamine stored in each vesicle. For both undifferentiated and differentiated cells the distributions of quantal size are approximated by one Gaussian, as determined by a normal probability distribution of cube root transforms represented by a straight line (data not shown), suggesting a single population of vesicles in each system. The distribution for undifferentiated cells is significantly narrower indicating that more large and small vesicles are present in differentiated cells.

Undifferentiated MN9D cells show little resemblance to dopaminergic neurons. However, in the presence of butyric acid for more than 6 days in culture, MN9D cells differentiate, showing a more neuronal morphology with a large flattened cell body and long processes, usually with multiple collateral branches. More recently, other stimuli, including retinoids, Nurr1, Bcl-2, and glial cell line-derived neurotrophic factor have been indicated to induce neurite outgrowth, DA synthesis, and storage, and cell cycle arrest in MN9D cells (Hermanson *et al.* 2003; Castro *et al.* 2001; Heller *et al.* 1996; Eom *et al.* 2004). In this experiment, not all the morphologically differentiated cells responded to high potassium stimulation. Morphological differentiation of MN9D cells is not always in accordance with function. It is important to note that although it is easier to detect amperometric spikes in differentiated MN9D cells (a higher percentage of differentiated cells show events), the number of events per cell in undifferentiated and differentiated cells is not significantly different among responsive cells. Butyric acid has been shown to alter cell morphology, growth, and gene expression. Recent data suggest that butyric acid changes electrophysiological profiles in MD9D cells. Butyric acid differentiated MN9D cells produced delayed rectifier potassium currents, high voltage-activated calcium currents, and transient sodium currents at significantly increased levels when compared with undifferentiated cells. However, in differentiated cells, the calcium and sodium currents are smaller, and no A-type potassium currents are present when compared with neurons acutely dissociated from the substantia nigra pars compacta (Rick *et al.* 2006). Therefore, the biochemical changes associated with butyric acid differentiation appear to drive MN9D cells to a more mature phenotype that can be used as a disease model.

In this study, both differentiation and L-DOPA can increase the quantal size and half-width. When comparing the half-width at relatively narrow-matched ranges ($Q^{1/3}$ from 30 to 40 molecules$^{1/3}$) for differentiation and L-DOPA, there is no significant difference, indicating that butyric acid and L-DOPA have no effect on extrusion of transmitter from the vesicle in MN9D cells. In PC12 cells, catecholamine stored in the halo is able to flow freely through the initial fusion pore (Alvarez de Toledo *et al.* 1993). After incubation in L-DOPA, most of the vesicular volume increase is in the vesicular halo, whereas the dense core swells relatively little

(Colliver *et al.* 2000). Interestingly, although butyric acid does not increase the vesicular volume, it decreases the size of dense core and leads to the increase in the vesicular halo. Thus, excess catecholamine would appear to be stored in the larger halo of differentiated cells, which is consistent with previous work where it was shown that DA loaded by L-DOPA is preferentially stored in the halo portion of PC12 cell dense core vesicles (Sombers *et al.* 2004).

The content of DA in the brain of PD patients is apparently decreased because of the loss of dopaminergic neurons. In the CNS, intercellular communication by DA requires diffusion-based volume transmission. Increased quantal sizes of DA in the surviving neurons can partially compensate the loss of dopaminergic neurons. Increasing quantal release of DA is a feasible and vital strategy for the treatment of PD. L-DOPA has been the most widely used and most effective drug for the symptomatic therapy of PD. Catecholamines are loaded into secretory vesicles by VMATs (Ahnert-Hilger *et al.* 2003). Two structurally related but pharmacologically distinct VMATs are known. Reserpine is a potent inhibitor of VMAT, which is believed to bind at the site of amine recognition. Our data show that treatment of differentiated MN9D cells with L-DOPA increases the quantal size. Reserpine blocks the increase in quantal size caused by L-DOPA. These results confirm that the changes in quantal size are VMAT-mediated. This is consistent with our previous results in PC12 cells (Colliver *et al.* 2000). Whether other substances such as glial cell line-derived neurotrophic factor can affect the quantal release of DA in MN9D cells need further investigation.

Previous studies with PC12 cells have shown that the average number of exocytosis events in the varicosities of differentiated cells is about 16 events per cell (Zerby and Ewing 1996). We show that for MN9D cells, an average of six amperometric events per cell follow stimulation of differentiated MN9D cells. The relatively fewer events present in the process of differentiated MN9D cells compared with differentiated PC12 cells might be explained by the presence of fewer LDCVs in the processes of differentiated MN9D cells or that the release probability in the two types of cells is different. In addition, single vesicles in differentiated PC12 cells contain an average of 106000 molecules, while the quantal size in differentiated MN9D cells is half that of the differentiated PC12 cells. MN9D cells are a fusion of mice mesencephalic neurons and the neuroblastoma cell line N18TG2. PC12 cells were derived from a pheochromocytoma of the rat adrenal medulla. In spite of the overall similarity in molecular composition and size between endocrinal and neuronal LDCVs, endocrine cells and neurons exhibit different profiles of transmitter release. In addition, there is evidence that endocrine cells and neurons exhibit various abilities to process, store, and secrete exogenous neuropeptides and peptide-processing enzymes (Marx *et al.* 1999). Because of the different origins of MN9D and PC12 cells, different catecholamine synthesis and storage machinery may be involved in MN9D cell and PC12 cells.

Besides LDCVs, catecholamine is also packaged in the SSVs in neurons. In cultured midbrain dopaminergic neurons, about 3000 molecules per quantum are released over 200 μs, much smaller and faster than quanta associated with LDCVs in MN9D cells (Pothos *et al.* 1998a). The diameters of LDCVs in MN9D cells are almost 110 nm, approximately twice as large as that of SSVs in dopaminergic neurons (40–60 nm). Therefore, more catecholamine is stored in the LDCVs and it requires more time to release neurotransmitters from LDCVs.

It is now established that neurons can secrete neuropeptides and neurotransmitters via at least two types of secretory organelles, i.e. the SSVs and the large dense-cored vesicles. To maintain synaptic transmission during intense neuronal activities, the synaptic vesicle pool at release sites is effectively replenished by recruitment of synaptic vesicles from the reserve pool and/ or by endocytosis. The fluorescent styryl dye, FM1-43, which incorporates into SSVs in nerve terminals during endocytosis and rejoins the nerve terminal during exocytosis, has been used

to monitor local vesicle recycling (Betz and Bewick 1992). In MN9D cells, catecholamine is packaged in the LDCVs and no obvious clusters of SSVs are seen.

The data presented here demonstrate that MN9D cells, when differentiated with butyric acid, increase quantal size and half-width significantly compared with undifferentiated cells. Catecholamines are stored in the LDCVs and can be modulated by DA pharmacology. Because of its mesencephalic origin, MN9D cells partially bridge the gap between pheochromocytoma cells and dopaminergic neurons, making them an appealing cell model to investigate mechanisms and potential therapeutics relevant to the quantal release of DA in PD.

Acknowledgements

Abbreviations

DA
  dopamine

LDCV
  large dense-core vesicle

NA
  norepinephrine

PD
  Parkinson's disease

SSVs
  small synaptic vesicles

VMAT
  vesicular monoamine transporter

References

Ahnert-Hilger G, Höltje M, Pahner I, Winter S, Brunk I. Regulation of vesicular neurotransmitter transporters. Rev Physiol Biochem Pharmacol 2003;150:140–160. [PubMed: 14517724]

Alvarez de Toledo G, Fernandez-Chacon R, Fernandez JM. Release of secretory products during transient vesicle fusion. Nature 1993;363:554–558. [PubMed: 8505984]

Betz WJ, Bewick GS. Optical analysis of synaptic vesicle recycling at the frog neuromuscular junction. Science 1992;255:200–203. [PubMed: 1553547]

Björklund A, Dunnett SB. Dopamine neuron systems in the brain: an update. Trends Neurosci 2007;30:194–202. [PubMed: 17408759]

Bruns D, Riedel D, Klingauf J, Jahn R. Quantal release of serotonin. Neuron 2000;28:205–220. [PubMed: 11086995]

Castro DS, Hermanson E, Joseph B, Wallén A, Aamisalo P, Heller A, Perlmann T. Induction of cell cycle arrest and morphological differentiation by Nurr1 and retinoids in dopamine MN9D cells. J Biol Chem 2001;276:43277–43284. [PubMed: 11553630]

Cavanaugh JE, Jaumotte JD, Lakoski JM, Zigmond MJ. Neuroprotective role of ERK1/2 and ERK5 in a dopaminergic cell line under basal conditions and in response to oxidative stress. J Neurosci Res 2006;84:1367–1375. [PubMed: 16941494]

Chen CXQ, Huang SY, Zhang LM, Liu YJ. Synaptophysin enhances the neuroprotection of VMAT2 in MPP^+-induced toxicity in MN9D cells. Neurobiol Dis 2005;19:419–426. [PubMed: 16023584]

Choi HK, Won LA, Kontur PJ, Hammond DN, Fox AP, Wainer BH, Hoffmann PC, Heller A. Immortalization of embryonic mesencephalic dopaminergic neurons by somatic cell fusion. Brain Res 1991;552:67–76. [PubMed: 1913182]

Colliver TL, Pyott SJ, Achalabun M, Ewing AG. VMAT-mediated changes in quantal size and vesicular volume. J Neurosci 2000;20:5276–5282. [PubMed: 10884311]

Colliver TL, Hess EJ, Ewing AG. Amperometric analysis of exocytosis at chromaffin cells from genetically distinct mice. J Neurosci Methods 2001;105:95–103. [PubMed: 11166370]

Eom DS, Choi WS, Oh YJ. Bcl-2 enhances neurite extension via activation of c-Jun N-terminal kinase. Biochem Biophys Res Commun 2004;314:377–381. [PubMed: 14733915]

Heller A, Price S, Won L. Glial-derived neurotrophic factor (GDNF) induced morphological differentiation of an immortalized monoclonal hybrid dopaminergic cell line of mesencephalic neuronal origin. Brain Res 1996;725:132–136. [PubMed: 8828597]

Hermanson E, Joseph B, Castro D, Lindqvist E, Aamisalo P, Wallén A, Benoit G, Hengerer B, Olson L, Perlmann T. Nurr1 regulates dopamine synthesis and storage in MN9D dopamine cells. Exp Cell Res 2003;288:324–334. [PubMed: 12915123]

Iversen SD, Iversen LL. Dopamine: 50 years in perspective. Trends Neurosci 2007;30:188–193. [PubMed: 17368565]

Lee YM, Park SH, Shin DI, et al. Oxidative modification of peroxiredoxin is associated with drug-induced apoptotic signaling in experimental models of Parkinson disease. J Biol Chem 2008;283:9986–9998. [PubMed: 18250162]

Marx R, Meskini RE, Johns DC, Mains RE. Differences in the ways sympathetic neurons and endocrine cells process, store, and secrete exogenous neuropeptides and peptide-processing enzymes. J Neurosci 1999;19:8300–8311. [PubMed: 10493731]

Mosharov EV, Sulzer D. Analysis of exocytotic events recorded by amperometry. Nat Methods 2005;2:651–658. [PubMed: 16118635]

Pothos EN, Davila V, Sulzer D. Presynaptic recording of quanta from midbrain dopamine neurons and modulation of the quantal size. J Neurosci 1998a;18:4106–4118. [PubMed: 9592091]

Pothos EN, Przedborski S, Davila V, Schmitz Y, Sulzer D. D2-like dopamine autoreceptor activation reduces quantal size in PC12 cells. J Neurosci 1998b;18:5575–5585. [PubMed: 9671649]

Rick CE, Ebert A, Virag T, Bohn MC, Surmeier DJ. Differentiated dopaminergic MN9D cells only partially recapitulate the electrophysiological properties of midbrain dopaminergic neurons. Dev Neurosci 2006;28:528–537. [PubMed: 17028430]

Robinson DL, Venton BJ, Heien ML, Wightman RM. Detecting subsecond dopamine release with fast-scan cyclic voltammetry in vivo. Clin Chem 2003;49:1763–1773. [PubMed: 14500617]

Sombers LA, Hanchar HJ, Colliver TL, Witterberg N, Cans A, Arbault S, Amatore C, Ewing AG. The effects of vesicular volume on secretion through the fusion pore in exocytotic release from PC12 cells. J Neurosci 2004;24:303–309. [PubMed: 14724228]

Sulzer D, Pothos EN. Regulation of quantal size by pre-synaptic mechanisms. Rev Neurosci 2000;11:159–212. [PubMed: 10718152]

Westerink RH, Ewing AG. The PC12 cell as model for neurosecretion. Acta Physiol (Oxf) 2008;192:272–285.

Zerby SE, Ewing AG. Electrochemical monitoring of individual exocytotic events from the varicosities of differentiated PC12 cells. Brain Res 1996;712:1–10. [PubMed: 8705289]

Zhang B, Adams KL, Luber SJ, Eves DJ, Heien ML, Ewing AG. Spatially and temporally resolved single-cell exocytosis utilizing individually addressable carbon microelectrode arrays. Anal Chem 2008;80:1394–1400. [PubMed: 18232712]
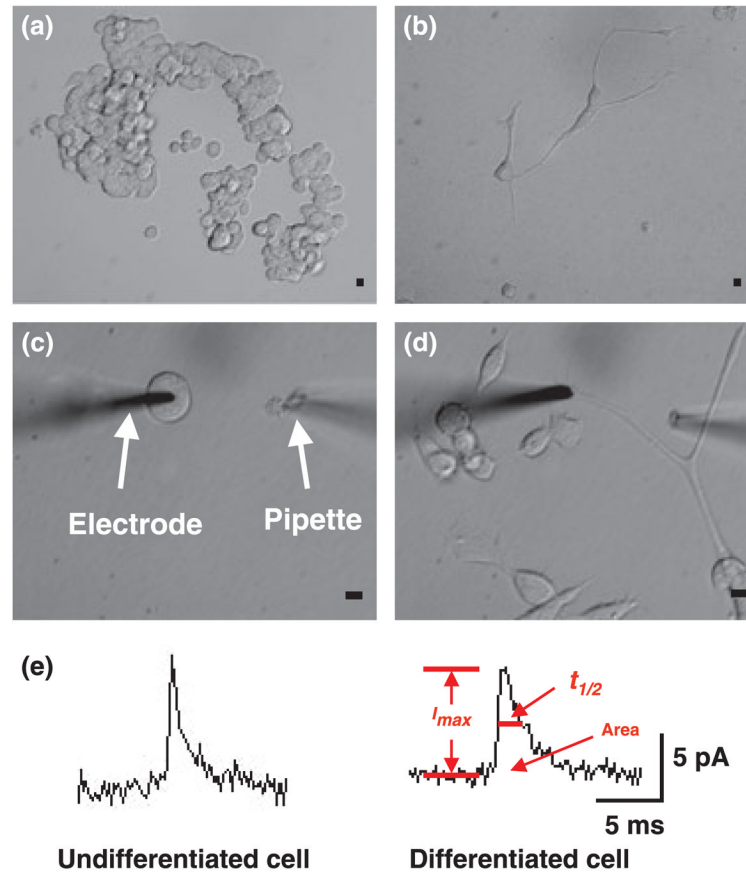
Fig. 1.
Morphology of MD9D cells in culture (a) undifferentiated MN9D cells cultured for 5 days. (b) Differentiated MN9D cells cultured for 7 days. (c) The electrode is placed on cell surface of undifferentiated MN9D cell. A microinjector is placed approximately 70 μm from the electrode. (d) The electrode is placed on process terminal of a differentiated MN9D cell. Scale bar = 10 μm. (e) Representative amperometric data from undifferentiated and differentiated MN9D cells. Area, $t_{1/2}$, and I_{max} were measured in the individual amperometric spikes. Peak area is defined as the time integral of each current transient, $t_{1/2}$ is the width of each peak at one-half of its height, and I_{max} is the height of each peak.
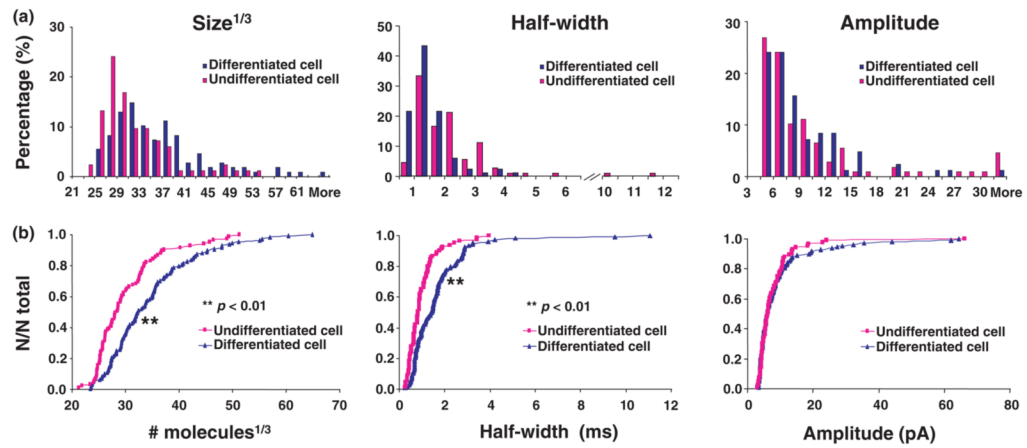
Fig. 2.
(a) Distributions of size$^{1/3}$, half-width, and amplitude in undifferentiated and differentiated MN9D cells ($n = 83$ events for undifferentiated group, $n = 106$ events for differentiated group).
(b) Cumulative histograms of size$^{1/3}$, half-width, and amplitude in undifferentiated and differentiated MN9D cells.
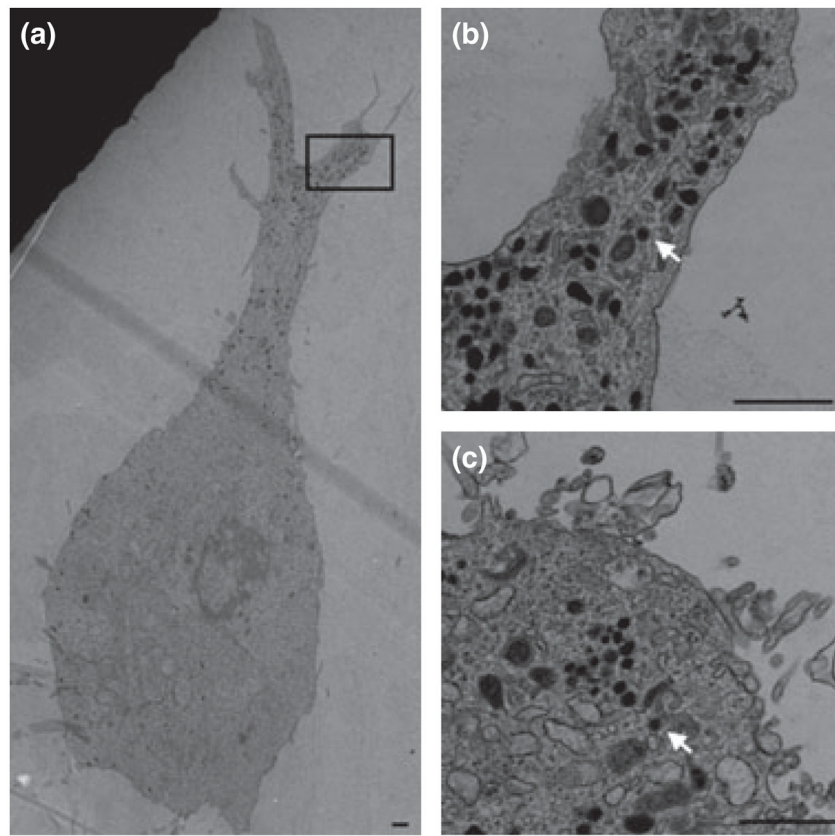
Fig. 3.
Electron micrograph of undifferentiated and differentiated MN9D cells. Large dense-core vesicles (LDCV, arrow) were mainly distributed in the process of differentiated cells (a). Panel b is the boxed area of panel a. LDCVs were also observed in cell body of undifferentiated cell (c). Scale bar = 1000 nm.
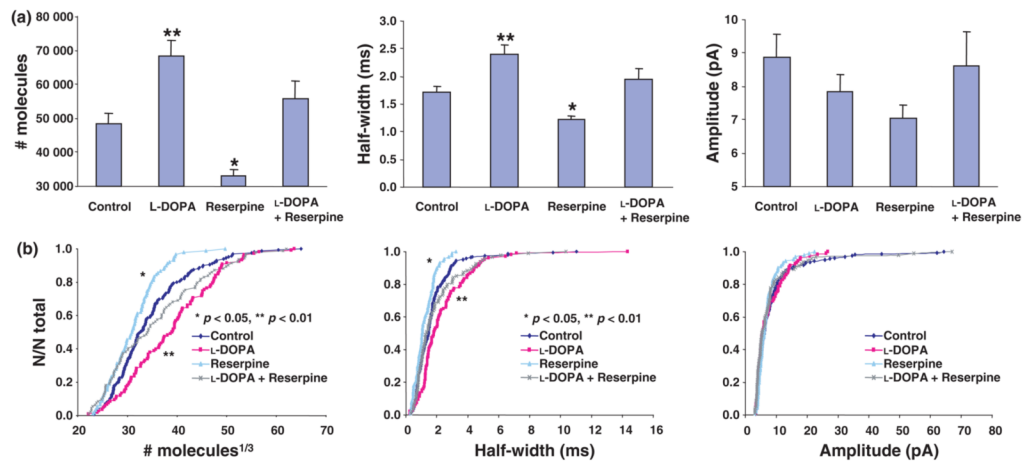
Fig. 4.
(a) Summary of number of molecules, half-width, and amplitude in differentiated MN9D cells with dopamine (DA) pharmacology ($n = 161$ events for control group, $n = 106$ events for L-DOPA group, $n = 90$ events for the reserpine group, and $n = 94$ events for L-DOPA + reserpine). $**p < 0.01$, $*p < 0.05$ versus control group. (b) Cumulative histograms of size$^{1/3}$, half-width, and amplitude in differentiated MN9D cells with DA pharmacology.